Identification of paleokarst by stable carbon and oxygen isotopes in Upper Jurassic carbonate rocks below the Molasse Basin

Martin E. Nowak
Bavarian Environment Agency, Hans-Högn-Straße 12, Hof/Saale

Keywords: Malm-Aquifer, Karst, Stratigraphy, Carbon Isotopes, Oxygen Isotopes, Moosburg SC4

Abstract

The Molasse Basin represents since several decades an important region for the production of geothermal energy. The high economic suitability of geothermal energy production in the Molasse Basin is based on favorable geologic conditions of the “Malm-Aquifer”, which represents a partly highly karstified succession of Upper Jurassic carbonate rocks, which are the main target for geothermal drillings. However, frequent changes of bedded and massive reef facies, which differ in diagenetic features like the degree of dolomitization and karstification as well as complex tectonic dissection, complicate geologic risk assessment. Intense karstification led to a high surface relief of the top of the “Malm-Aquifer” and complicates stratigraphic classification of drilling samples, especially cuttings. In turn, karstified areas, especially in the upper position of the profile, provide excellent flow conduits for geothermal water production. In order to develop new geochemical tools for stratigraphic classification, as well as to recognize karstified areas from drilling samples, we investigated the application of stable carbon and oxygen isotopes for distinguishing between different lithostratigraphic units as well as due to karstification recrystallized sections. Therefore, we calibrated a chemostratigraphic curve based on stable carbon and oxygen isotope measurements of bulk rock samples the Moosburg SC4 core, a drilling core representing the whole Upper Jurassic succession of the eastern Molasse Basin. First results show that lithostratigraphic formations of the lower and middle section of the Upper Jurassic as well as different dolomite types can be distinguished based on their $\delta^{13}C$ and $\delta^{18}O$ isotopic signature. In the lowest section, between 1570 and 1530 m bgl $\delta^{13}C$ and $\delta^{18}O$ of bulk rock samples values increase from around -0.7 to around +3 permille and from -6 to 0 permille V-PDB, respectively. This section is represented by the Sengenthal and lower Dietfurt formations of the Callovian and Oxfordian stage, repectivley. During the Kimmerdigian, both isotopes show a shift towards more depleted values again of around -2 permille in $\delta^{13}C$ and -4 to -2.5 permille in $\delta^{18}O$. Dolostones from different stratigraphic units (Sengenthal formation and Frankenalb formation) can also be distinguished according to their $\delta^{13}C$ and $\delta^{18}O$ values. Highly karstified sections can be distiguished from not karstified sections by lower $\delta^{13}C$ values and more uniform $\delta^{18}O$ values, as indicated by measurements of karstified samples from a Tithonian reef complex drilled out in the Weika 19, Pfahldorf core. I hypothesize that this signature is indicative for sections of the Malm aquifer under the Molasse Basin, which was karstified under meteoric vadose conditions in early Cretaceous and Tertiary times.

1. Introduction

Climate change is one of the greatest challenges facing humanity in the coming decades. In the Paris Agreement, 197 countries declared their willingness to limit global warming to 1.5°C and to be CO_2-neutral by 2050. Together with other European countries, Germany has declared that it will reduce CO_2 emissions by 40% by 2030 compared with 1990 levels, which means a reduction of 175 mio to 183 mio tonnes of CO_2/Äq. in the energy sector[1]. Renewable energies are regarded as the most promising strategy for a permanent abolition of CO_2-intensive coal-fired power generation[1].

[1] Klimaschutzprogramm 2030 der Bundesregierung zur Umsetzung des Klimaschutzplans 2050: https://www.bmu.de/fileadmin/Daten_BMU/Download_PDF/Klimaschutz/klimaschutzprogramm_2030_umsetzung_klimaschutzplan.pdf Webseite angefordert am 08.11.2019.

The Molasse Basin in Southern Germany is one of the most promising regions for deep geothermal power and heat generation (Fritzer et al., 2010). Deep geothermal (DG) energy is an eternal source of electricity and heat in human life spans. DG uses deep boreholes with water temperatures of 40 to 100 °C, while power generation is possible from temperatures of about 80°C (Fritzer et al., 2010). In the Molasse Basin, the "Malm-Aquifer" is the most promising target for energy and heat generation (Fritzer et al., 2010; Böhm et al., 2011; Birner, 2013; Beichel et al., 2014; Koch & Munnecke, 2016). It is a predominantly carbonate-dominated Upper Jurassic sequence of up to 600 m thickness. The Malm aquifer was affected by intensive karst formation from the early Cretaceous to the Tertiary. Since the early Eocene, the Malm Aquifer has been involved in the mountain foredeep formation of the Molasse Basin, which has been gradually filled with Tertiary sediments (Bader et al., 2003; Unger, 1996; Bachmann et al., 1987; Lemcke, 1977; Elberskirch & Lemcke, 1953). Successful geothermal exploitation depends on different geological conditions such as facies type, tectonic disturbances and diagenetic features such as dolomite formation or karstification (e.g. Fritzer et al., 2010; Böhm et al., 2010; Birner, 2013). This paper focuses on karst as a favorable feature of the Malm aquifer for geothermal energy production and gives an overview of the karst history of the Upper Jurassic in the South German Molasse Basin. I also provide a proposal for the use of geochemical proxies to identify sections affected by intensive karstification. I calibrated isotopic fingerprints of ltihostratigraphic units of the Upper Jurassic under the Molasse Basin on a drill core representing the entire sequence, the Moosburg SC4 drill core, and a core subjected to intense karstification, the Weika 19, Pfahldorf core. Such data could provide helpful proxies to evaluate the contribution of karst to water production in the Malm-Aquifer.

1.1 Stratigraphy of the Malm Aquifer

The "Malm Aquifer" consists mainly of carbonate rocks of the “Weißjura” group, an Upper Jurassic supergroup deposited between 156 and 142 Ma on a gently south-facing carbonate ramp on the northern shelf of the Tethys (Meyer & Schmidt Kaler, 1989; Meyer, 1996). The Upper Jurassic in Southern Germany can be divided into two predominant facies types, a bedded facies comprising well bedded limestones with embedded marls and a reef facies consisting predominantly massive and often dolomitized carbonate rocks. The bedded facies can be further subdivided into a well bedded facies of the lower Weißjura, which is a subtidal facies in an outer ramp setting and a Plattenkalk facies of the upper Weißjura, deposited in shallow intertidal basins between reefs on carbonate platforms (Ruf et al., 2006; Koch et al., 2010, Kröner et al., 2017). The bedded facies of the lower section is represented by the Impressamergel-, Wohlgeschichtete Kalke- and Lacounosamergel formations in the western part and the Dietfurt- and Arzberg-Formation in the eastern part of the basin (Koch et al., 2010; Niebuhr & Pürner, 2014; Nowak et al., 2018). The thickness of the bedded facies in the lower Weißjura group can be up to 130 m in the western part and up to 100 m in the eastern part of the Molasse Basin. A special feature within the Weißjura group is the occurrence of a sponge megafacies, the Frankenalb formation, which can reach a thickness of up to 150 to 200 m. Starting from first isolated reef bodies in the Oxfordian, the Frankenalb Formation had its biggest extent in the Upper Kimmeridgian where it formed a pancreatic sponge-algal platform of the Franconian/South Bavarian platform in the east and a Swabian Reef platform in the western shelf. Both platforms where divided by a NE-SW striking basin with predominantly marly bedded facies (Meyer & Schmidt Kaler 1989, Koch et al., 2010). On the Franconian-South Bavarian platform, the Frankenalb formation is characterized by a high degree of dolomitization (Reinhold, 1998). In the course of a general regression in the Tithonian, the sponge megafacies disapeared and gave way to the increasingly prominent Plattenkalk facies deposited in shallow basins between the reef bodies (Mayer & Schmidt-Kaler 1989). In the area of Southern Bavaria a shallow water sponge coral platform with ooid shoals and stromatolitic algae occurrences as well as abundant Plattenkalk basins was developed. Sediment thickness of Upper Kimmeridgian to Tithonian strata can reach thicknesses of up to 350 m. In the Lower Cretaceous, the sea regraded again and the entire platform was subjected to enduring karstification under tropical conditions (Lemcke, 1987).

1.2 Karstification of the Malm plateau and implications for drilling processes

A first karst period most probably already affected the Upper Jurassic strata during a regressive cycle in the Upper Kimmeridgian (Pomoni-Papaioannou et al.,1989; Birner, 2013). After the final retreat of the Tethyan Sea in the lower Cretaceous period, the Upper Jurassic plateau underwent several further karst periods. In the Molasse Basin east of Munich, karst formation on the Upper Jurassic plateau began immediately after the last regression of the Tethyan Ocean and for more than 40 million years mainly affected the NE part of the so-called "Ostbayerische Randsenke". Several hundred metres of Jurassic sediments were already eroded in this first karst period (Lemcke, 1987). Two repeated transgression cycles in the Lower and Upper Cretaceous impeded further karst formation in this area and led to the deposition of predominantly marine shale and sand deposits on top of the karst (Lemcke, 1987, Bachmann et al., 1987) (Fig. 1).
In the western part of the Molasse Basin west of Munich, karstification lasted from the Lower Cretaceous to the Upper Cretaceous uninterrupted for more than 70 million years, until the deposition of marine sediments by the first Cenomanian transgression. Due to a successive inclination of the layers towards SSE, the karst formation most probably influenced the Upper Jurassic plateau to a depth of 200 to 300 m below its hanging wall (Lemcke, 1987). In the area between the Lech and Isar rivers, karst formation in the Upper Eocene was reintroduced for 30 million years after the erosion of the Cenomanian deposits (Lemcke, 1987).
In the area west of the Lech river karstification was attenuated as the first terrigenous sediments of the "Untere Süßwassermolasse" covered the exposed surface of the Upper Jurassic (Fig. 1). The sedimentation of the "Untere Süßwassermolasse" in the western Molasse Basin lasted from the Upper Eocene to the Lower Miocene, followed by a stop of the terrigenous sedimentation, which was accompanied by the regression of the "Untere Meeresmolasse" in the eastern part of the Molasse Basin. The sedimentation stopped for about 5 million years and most probably exposed parts of the Upper Jurassic surface of the Upper Jurassic (Lemcke, 1987). This karst period was successively stopped by covering the exposed parts of the Upper Jurassic surface with sediments of the "Obere Meeresmolasse", which transgraded the entire Molasse Basin up to a shore line at the southern edge of the Franconian and Swabian Alb. Subsequently, the following "Obere Süßwassermolasse" covered the basin in the Upper Miocene and even parts of the adjacent plateau of the Franconian and Swabian Alb with terrigenous sediments by a river system from the eastern hinterland (Lemcke, 1987; Lemcke, 1977).
Important events influencing the karst of the Upper Jurassic Malm Aquifer during the Miocene were the incision of the "Graupensandrinne" in the Lower Miocene and its subsequent backfilling with siliceous sediments of the "Obere Süßwassermolasse", accompanied by an adaptation of the pressure water level of the northern Malm Aquifer to the receiving waters along the northern edge of the Molasse Basin (Lemcke 1987; Lemcke 1977; Lemcke & Tunn 1956). The incision of the Danube into the Upper Jurassic plateau in the Pliocene led again to new hydraulic conditions of the Malm aquifer and to the reactivation of old karst structures (Lemcke, 1987).
The Schwabmünchen, Füssing 1 and Birnbach 1 wells (Cramer, 1953; Lemcke & Tunn, 1956; Lemcke, 1987) provided the first indications of the productivity of paleokarst in the South German Molasse Basin. Karst cracks and cavities usually lead to the loss of drilling mud or the fall through of drill pipes, which can lead to considerable geological risks and economic losses (Lemcke, 1987; Fritzer et al., 2010; Böhm et al., 2010). Such technical problems can affect drilling processes to a depth of approx. 350 to 400 m below the hanging wall of the Malm Aquifer (Lemcke, 1987). Lemcke (1987) assumed that the probability of opening paleokarst by drilling is higher in the Molasse Basin east of the Lech. Although there the karstification lasted less time, the higher abundance of massive reef facies led to a more even distribution of paleokarst in this area. Although the karst formation in

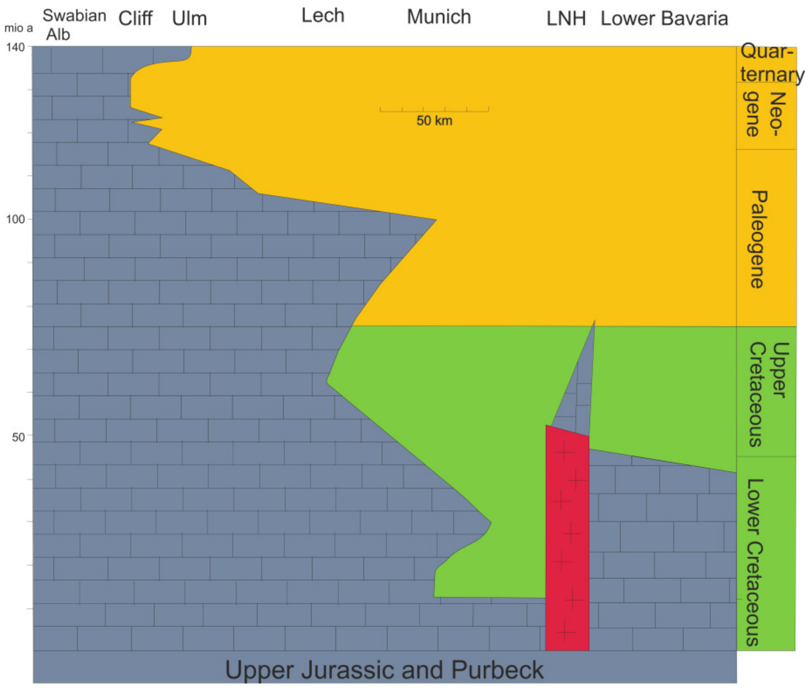

Fig. 1: Schematic distribution of Paleokarst affecting the Upper Jurassic plateau. Modified after Lemcke (1987).

the western Molasse Basin lasted longer, the higher proportion of bedded facies led to a lower frequency of widely connected karst structures in this area (Lemcke, 1987). Given the extent of paleokarst and its potential importance for drilling processes, tools for the timely identification of paleokarst and the associated geological risk assessment are urgently needed. Stable isotopes can provide a helpful proxy to assess the origin and diagenetic history of carbonate rocks (Weissert & Erba, 2004; Nowak et al., 2018).
The isotope ratio of a sample is expressed as the deviation of the $^{13}C/^{12}C$ ratio of a sample compared to the $^{13}C/^{12}C$ ratio of a reference standard, usually the Vienna PeeDee Belemnite (V-PDB), in permille:

$$\delta^{13}C = \left[\frac{\frac{^{13}C_{Sample}}{^{12}C_{Sample}}}{\frac{^{13}C_{Standard}}{^{12}C_{Standard}}} - 1 \right] \times 1000 \; [permilleV - PDB] \qquad [1]$$

Carbon and oxygen isotopes of carbonates generally represent the carbon and oxygen isotope composition of dissolved inorganic carbon of seawater during deposition as well as recrystallisation and calcite precipitation processes during diagenesis (Bathhurst, 1975; Allan & Matthews, 1982). Under certain circumstances, carbon and oxygen isotopes of both, bulk and compound specific components of carbonate rocks can be used to reconstruct paleo-ecological conditions of depositional systems (Weissert & Erba., 2004). The aim of this study was to distinguish between different lithostratigraphic units of the Moosburg SC4 drill core (Meyer, 1994) using carbon and oxygen isotopes from bulk carbonate rocks and to compare the results with the strongly karstified Weika 19, Pfahldorf core. I assumed that differences in the paleo-environmental conditions in the lower part of the Upper Jurassic caused differences in the isotopic composition of the different lithostratigraphic units. In the upper section, changing diagenetic characteristics such as dolomitization and different cementation events can cause isotopic changes in different sedimentological units. Finally, meteoric vadose diagenesis and the associated karst formation should generate a signal that clearly differs from unkarstified sections (Nowak et al., 2018).

2. Materials and methods

Bulk rock samples of approx. 5 cm thickness were taken from the two drill cores for isotope analysis. The Moosburg SC-4 core, which represents the entire Upper Jurassic succession in the eastern Molasse Basin (Meyer, 1994) (Fig. 2 & Fig. 3), was sampled every three meters and every 20 cm at lithological transitions. The Weika 19, Pfahldorf core represents a drill core through a strongly karstified section of an Upper Tithonian sponge reef complex of the Southern Franconian Alb (Fig. 2 & Fig. 3). Sampling was the same as for the Moosburg SC4 core.
After sampling, the samples were ground with an agate ball mill, sieved to 63 microns and air-dried. 130 samples were taken from the Moosburg SC4 core, covering ½ of the drill core, and 73 samples were measured. 9 samples were collected from the Weika 19, Pfahldorf core.
400 to 500 µg of carbonate powder were weighed into Exetainer® borosilicates, which were then sealed with butyl rubber septa screw caps. Exetainers were rinsed with nitrogen for 3 minutes in an automated autosampler. The samples were acidified manually with three droplets of 104% phosphoric acid and placed in a heated rack at a constant temperature of 80°C. The samples were then rinsed with nitrogen for 3 minutes. The measurements were started after one hour of reaction. NBS 18 and IAEA-603 were used to perform a two-point calibration. The normalized carbon isotope ratios of the samples are expressed in permille relative to the V-PDB standard. Fractionation factors for acid fractionation were obtained from Rosenbaum and Sheppard (1988) and are normalized for fractionation at 25°C.
Isotope ratios are given as $\delta^{13}C$ value, i.e. the deviation of the $^{13}C/^{12}C$ ratio of the sample from the ratio of the Vienna V-PDB standard in permille according to equation 1. Errorbars represent 1 sigma standard deviation of three replicates of one core sample. Statistical analyses were conducted with R-statistics with the “stats” and “car” packages (Fox et al., 2012).

3. Results

3.1 Results of isotope measurements

Fig. 4 shows $\delta^{13}C$ and $\delta^{18}O$ results of carbonates from the different lithostratigraphic formations of the Moosburg core. The lower part of the profile shows characteristic changes with depth. The $\delta^{13}C$ values shift from -0.7 permille to +1.8 permille in the lowest section of the profile, the Sengenthal formation. A similar shift can be observed in $\delta^{18}O$, where the values shift from about -5 permille to -1.8 permille. This trend in both isotopes continues into the lower part of the oxfordian Dietfurt formation. The values of $\delta^{13}C$ and $\delta^{18}O$ both shift towards more depleted values in the kimmeridgian Arzberg formation (Fig. 4). In the Arzberg formation $\delta^{13}C$ values show signatures of about +2 permille and $\delta^{18}O$ values shift up to -4 permille. Within the dolomitized section of the lower Frankenalb Formation, both $\delta^{13}C$ and $\delta^{18}O$ scatter between values of 1.1 to 2.7 permille and -6.8 and -2.4 permille, respectively. In the upper part of the Frankenalb formation, between about 1430 and 1420 m bgl, $\delta^{18}O$ still shows scattering values of -3.1 to -4.6 permille, while $\delta^{13}C$ remains relatively stable with a value of about 2.3 to 2.8 permille. Data from Tithonian strata is not available, yet.
Samples from the Weika 19, Pfahldorf core show very different results in $\delta^{13}C$, but not in $\delta^{18}O$. $\delta^{13}C$ varies around -7.6 and -8.3 permille and $\delta^{18}O$ values scatter within a narrow range of -4 to -4.5 permille.
Fig. 5 shows a scatter diagram of $\delta^{13}C$ versus $\delta^{18}O$. Karstified samples clearly plot outside the range of unkarstified samples.

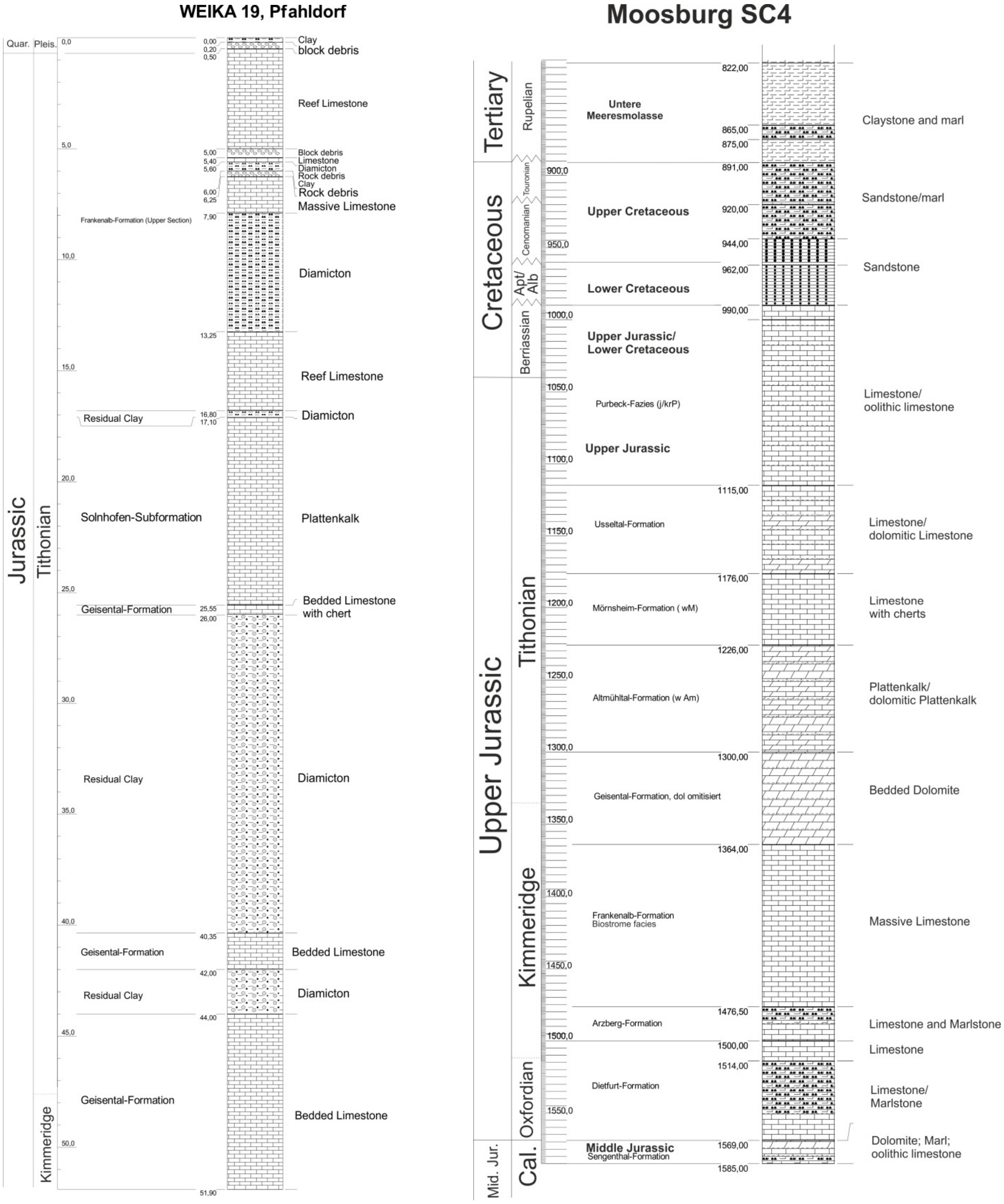

Fig. 2: Lithologic and stratigraphic succession of the Weika 19, Pfahldorf core and the Moosburg SC4 core.

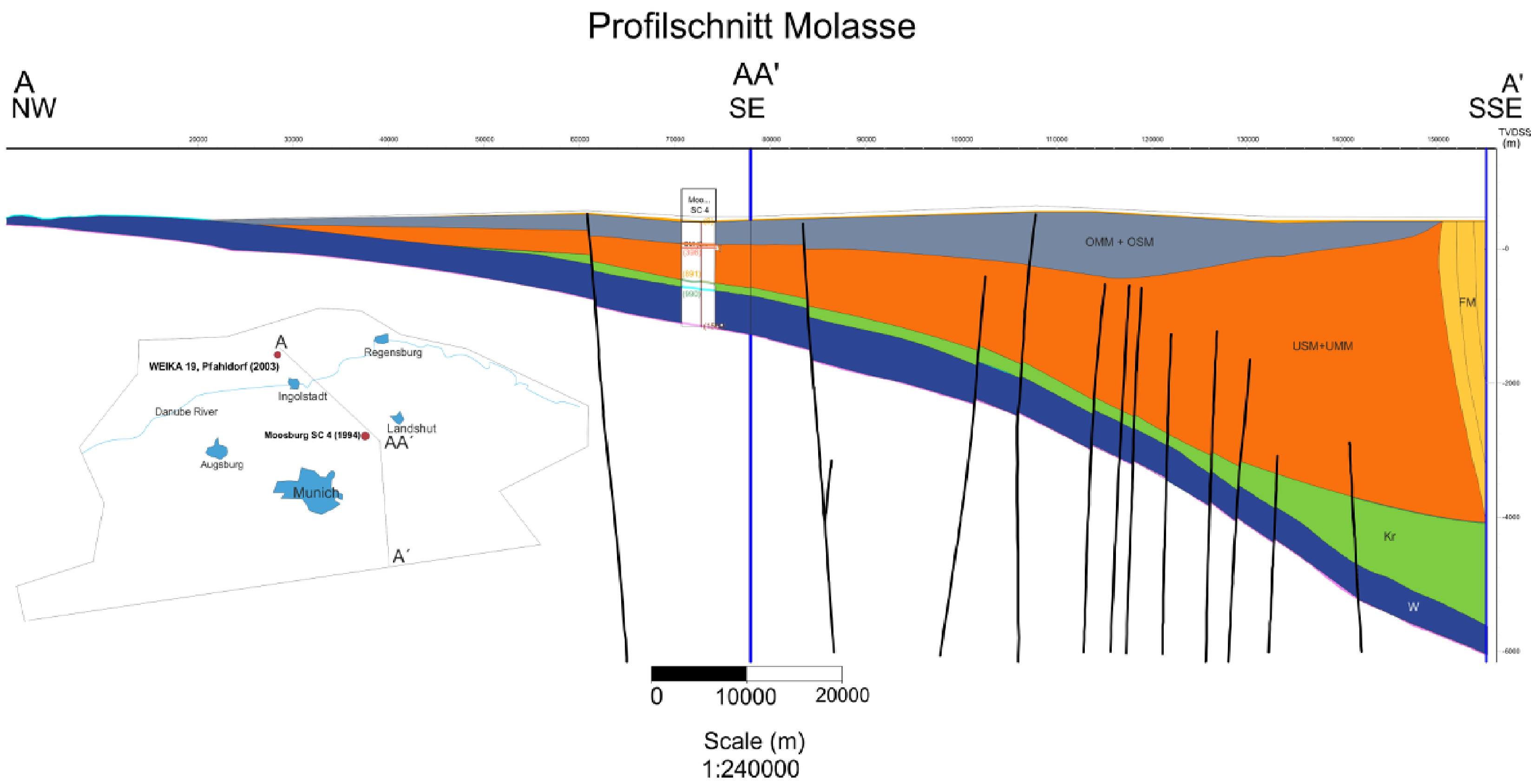

Fig. 3: Schematic cross-section through the Molasse Basin and location of the Moosburg drilling core. Location of the Weika 19 core is indicated in the overview map. OMM + OSM = Obere Meeresmolasse and Obere Süßwassermolasse; USM+UMM Untere Süßwassermolasse und Untere Meeresmolasse; Kr = Cretaceous; w = Upper Jurassic; FM = Faltenmolasse

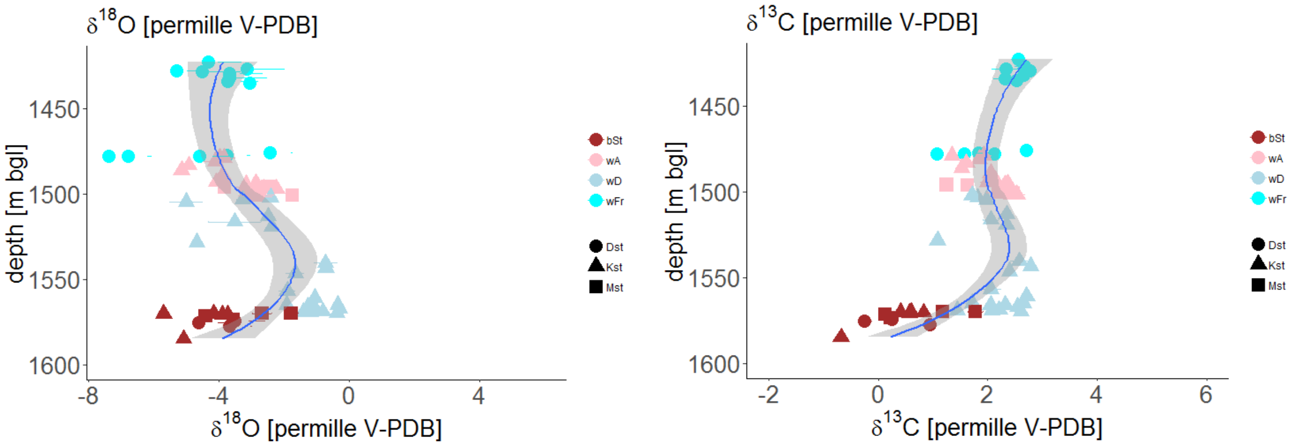

Fig. 4: Results of the isotope measurements along the Upper Jurassic succession of the Moosburg drilling core. Both isotopes show systematic changes along the depth profile from Callovian until Kimmeridgian strata. Blue line represents a locally weighted regression model and grey bands its 95% confidence interval. Sample values represent the mean of three repeated measurements of a sample taken from the respective drill core section and error bars its 1 sigma standard deviation.

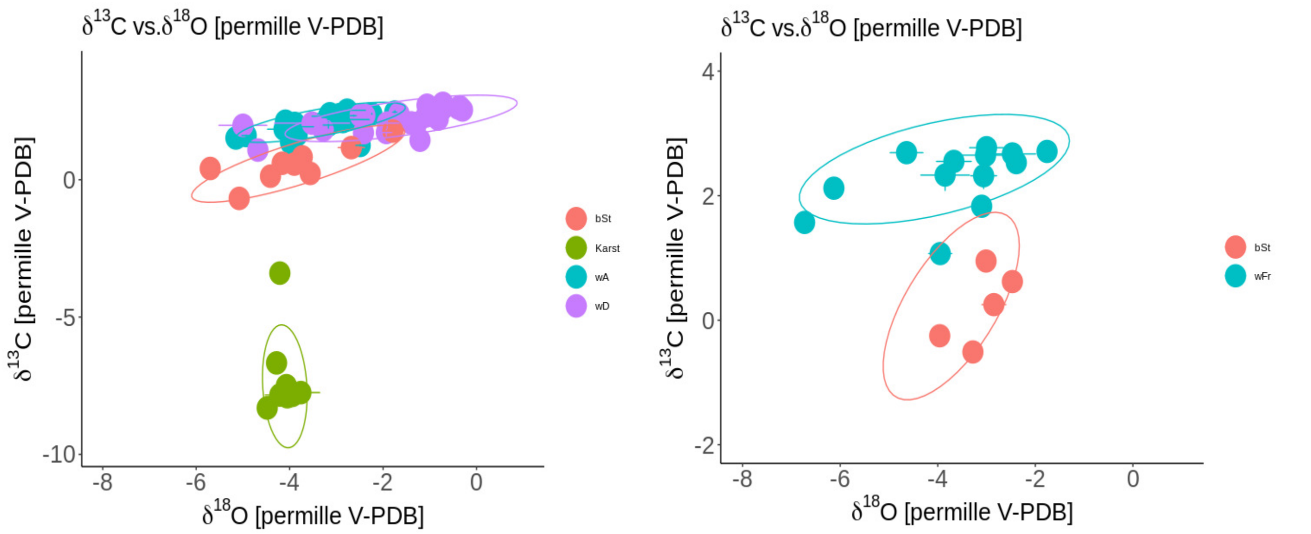

Fig. 5: Scatter plot of $\delta^{13}C$ vs $\delta^{18}O$ values with confidence ellipses at 90 % confidence level. Error bars represent the standard deviation from the mean of three replicated measurements. All lithological formations of the Moosburg drilling core can be separated according to their lithology and stable isotopic values. Additionally, karstified samples from the Weika 19, Pfahldorf core exhibit more depleted $\delta^{13}C$ compared to the Moosburg core. Also different dolomite generations of the Moosburg core can be distinguished according to their isotopic signature. bSt=Sengenthal Fm; wD=Dietfurt Fm; wA=Arzberg Fm; wFr=Frankenalb Fm; Karst=Weika 19 core samples.

4. Discussion

4.1 Application of stable isotopes for stratigraphic classification of Upper Jurassic carbonates

Both, $\delta^{13}C$ and $\delta^{18}O$ isotopes show distinct trends with depth. As has been shown earlier (Nowak et al., 2018), $\delta^{18}O$ values are predominantly controlled by the lithology of the rock. Biggest changes in

$\delta^{18}O$ are caused by dolomitization, which can strongly affect the oxygen isotopic composition of Upper Jurassic carbonate rocks (Reinhold et al., 1998). $\delta^{18}O$ but not $\delta^{13}C$ values of Oxfordian and Lower Kimmeridgian strata, i.e. Dietfurt and Arzberg Formations, show a linear correlation with gamma ray values (R-squared = 0.45, p-value >0.05 and R-squared = 0.01747, p-value = 0.4162). This might indicate isotope exchange reactions of pore water with clay minerals during early diagenesis of the strata (Dickson & Coleman, 1980) (Fig. 6). However, the pronounced shift of both, $\delta^{13}C$ and $\delta^{18}O$ values during the transition from Callovian to Oxfordian at 1659 m bgl. is certainly influenced by climatic and oceanographic transitions during sedimentation (Ruf et al., 2005, Weissert & Erba, 2004).
Using $\delta^{13}C$, $\delta^{18}O$ and lithology, all lithostratigraphic units of Oxfordian and Kimmeridgian strata of the Moosburg SC4 core can be distinguished. Also the different dolomite types of the Sengenthal

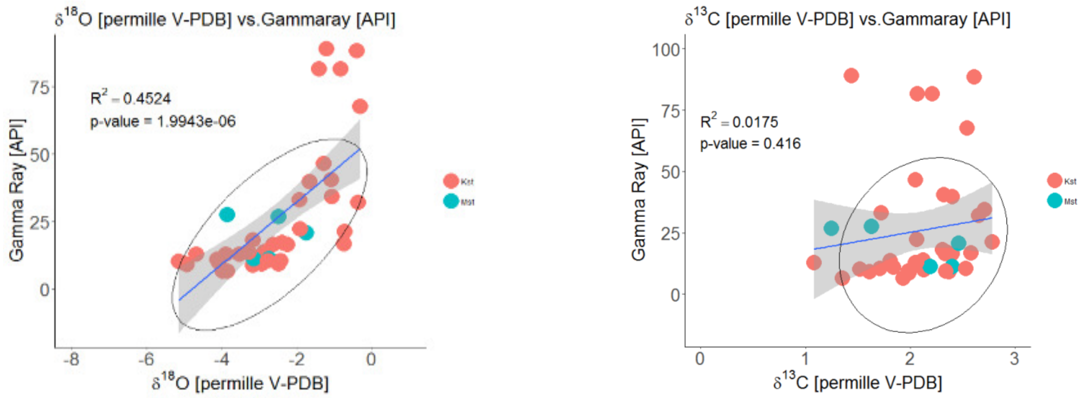

Fig. 6: Correlation of isotope signatures with gamma ray values from the lower section of the drill core. Data includes samples from the Dietfurt Formation and Arzberg Formation. $\delta^{18}O$ values show a significant correlation with gamma ray values (blue line; grey bars indicate 90% confidence intervals of the linear model), whereas $\delta^{13}C$ values are not correlated with gamma ray. Kst=limestone; Mst=Marlstone. Values outside the 90% confidence ellipses represent samples from the base of the Upper Jurassic, a glauconitic bed @ 1569 m bgl.

Formation and the Frankenalb Formation can be distinguished by their $\delta^{13}C$ and $\delta^{18}O$ ratios. Figure 5 clearly shows that the karstified areas of the Weika 19, Pfahldorf core scatter outside the range of the not karstified limestone and dolomite samples of the Moosburg core.
Karst is usually caused by water rock interactions, which manifest themselves through dissolution, precipitation and ion exchange processes. It is mainly driven by water loaded with carbon dioxide from soil CO_2 (Nowak et al., 2017). Processes that influence the isotopic composition of DIC and aquifer rock are summarized in Nowak et al. (2017). The most important isotope exchange reactions can be characterized according to:

$$CO_2 + H_2O + CaCO_3 \rightarrow Ca^{2+} + 2HCO_3^- \quad [2]$$

which represents dissolution of the carbonate rock,

$$C^*O_2 + HCO_3^- \leftrightarrow CO_{2(g)} + HC^*O_3^- \quad [3]$$

representing ionic exchange between soil CO_2 and DIC and

$$HC^*O_3^- + CaCO_3 \leftrightarrow HCO_3^- + CaC^*O_{3(s)} \quad [4]$$

which is ionic exchange between DIC and carbonate rock.

Soil CO_2 under C3-vegetation is characterized by a $\delta^{13}C$ value of around -23 permille, whereas carbonates have a much more ^{13}C enriched value of around 0 to 2 permille (Nowak et al., 2017).

The extent of the isotopic exchange depends on the mineralogy of the carbonate rock, DIC concentration and temperature (Wigley, 1976).
When water loaded with soil CO_2 gets in contact with carbonate rock, DIC gets diluted according to equation 2 and the isotopic value changes according to (Han & Plummer, 2012):

$$^{13}C_0 = \left(\frac{C_a}{C_t}\right) \times {}^{13}C_g + 0.5\frac{C_b}{C_t}\left({}^{13}C_g + {}^{13}C_s\right) \qquad [5]$$

where $^{13}C_0$ represents the $\delta^{13}C$ value of DIC reacting with $CaCO_3$, C_a, C_b and C_t refer to $CO_{2(aq)}$, HCO_3^- and total DIC concentrations, respectively. $^{13}C_g$ and $^{13}C_s$ refer to $\delta^{13}C$ values of soil gas and carbonate, respectively.
Since DIC gets usually diluted by $CaCO_3$ in a 1:1 ratio according to equation 2 and carbonates are characterized by $\delta^{13}C$ values of around 0 permille, DIC in limestone aquifers gets enriched in $\delta^{13}C$ by about +10 permille (Tamers, 1975).

The impact of isotopic exchange between DIC and carbonate rocks for their $\delta^{13}C$ can be described according to following equation (Han & Plummer, 2012):

$$\delta^{13}C_0 = \left(\frac{C_a}{C_t}\right) \times \left(\delta^{13}C_s - \varepsilon_{s/a}\right) + \left(\frac{C_b}{C_T}\right) \times \left(\delta^{13}C_s - \varepsilon_{s/b}\right) \qquad [6]$$

Where $\varepsilon_{s/a}$ and $\varepsilon_{s/b}$ refer to carbon isotope discrimination between $CaCO_3$ and $CO_{2(aq)}$ and $CaCO_3$ and HCO_3^-, respectively. As can be derived from equation 4, isotopic exchange affects both, DIC of the percolating water and the carbonate rock in a 1:1 molar ratio, whereas $\delta^{13}C$ values of DIC get shifted towards more enriched and the carbonate rock towards more depleted values.
The $\delta^{13}C$ value of the carbonate rock can be therefore indicative for the identification of paleokarst, as is also reflected in the samples from the Weika 19, Pfahldorf core. Regarding the long exposure time of the Malm Plateau as well as the prevailing climatic conditions, which were tropical during the karstification period, a high degree of recrystallization and ionic exchange seems plausible (Lemcke, 1987). Stückl (2003) investigated a fossil Karst relief of the Upper Jurassic plateau in the vicinity of Regensburg, which was subsequently covered by Miocene strata. Relief differences can amount up to 70 m and can be further increased by tectonic displacement (Stückl, 2003).
This high degree of karstification can also be expected for the upper layers of the Malm Aquifer below the Molasse Basin (Lemcke, 1987). Pomoni-Papaioannou et al. (1989) described a high degree of recrystallisation in an Upper Jurassic sequence of a drill core in the western Molasse Basin. The authors found recrystallization patterns by microfacies analysis to a depth of 100 m below the hanging wall of the Malm aquifer, which are attributed to Cretaceous and Tertiary karstification (Pomoni-Papaioannou et al. 1989). Birner (2013) also describes two karstification horizons in the Malm-Aquifer, a lower horizon in Upper Kimmeridgian layers of the Frankenalb formation about 200 to 300 m below the hanging wall, representing the peak of the Upper Jurassic regression cycle, and a karstic section in the Tithonian layers mainly representing meteoric weathering during the Lower Cretaceous and Tertiary. Both horizons differ in their manifestations. The lower karst horizon is usually characterized by a porous facies several meters thick, with a high lateral and uniform extent (Birner, 2013, Böhm, 2011). The upper karst horizon is characterized by a high degree of dedolomitization and the formation of cone structures as well as the occurrence of residual clays or sand sediments.
Samples from the Weika 19, Pfahldorf core represent the later karst type, which is characterized by a high degree of recrystallization, the occurrence of sinter structures and the disintegration of

dolomitized areas and dedolomitization (Fig. 2). Dedolomitization is typically associated with a decrease in $\delta^{13}C$ values due to recrystallization and isotopic exchange according to equations 4 and 6. In addition, the $\delta^{18}O$ values of carbonates exposed to meteoric vadose diagenesis tend to show a more even distribution of $\delta^{18}O$ values (Allan & Matthews, 1982). This also applies to samples from the Weika 19, Pfahldorf core (Fig. 5).
The Moosburg core has two horizons corresponding to a highly porous facies, at about 1450 and 1430 m bgl and between 1420 and 1360 m bgl (Böhm et al., 2011). Isotope signatures within these sections are characterized by significantly more enriched $\delta^{13}C$ and $\delta^{18}O$ compared to the Weika 19 core, while areas with abundant vugy porosity within the core generally have more depleted $\delta^{13}C$ values than samples outside the porous facies. This may be an indication of the influence of meteoric phreatic diagenesis, but is also difficult to distinguish from different dolomitization phases (Reinhold, 1998). Since dolomitic facies in the section between 1462 m to 1364 m show a generally uniform appearance, a meteoric diagenetic overprint appears also plausible.

Conclusions

The Malm-Aquifer is the most important aquifer for geothermal applications in the Molasse Basin. Permeabilities and flow rates of the Malm aquifer are highly dependent on diagenetic characteristics such as dolomitisation and karstification, which affected the Malm aquifer in a short synsedimentary phase already in the Upper Jurassic and for several million years since the Lower Cretaceous. Stable carbon and oxygen isotope signatures of limestones and dolostones provide a suitable tool to distinguish between the two karstification periods. Meteoric vadose karst phases are characterized by depleted $\delta^{13}C$ values and uniform $\delta^{18}O$ values. Sections which are likely influenced by meteoric phreatic karst sections generally have more enriched $\delta^{13}C$ values than meteoric vadose samples and show a generally higher variability in $\delta^{18}O$. The results indicate that stable carbon and oxygen isotopes might offer the possibility to distinguish between different types of the Malm aquifer below the Molasse Basin and might be a tool for water provenance, which has to be further evaluated.

References

ALLAN, J.R. & MATTHEWS, R.K. (1982): Isotope Signatures associated with early meteoric diagenesis. – Sedimentology, 29: 797-817.

BACHMANN, G.H., MÜLLER, M. & WEGGEN, K. (1987): Sedimentary and structural evolution of the German Molasse Basin. – In: P.A. Ziegler (Ed.): Compressional Intra-Plate Deformations in the Alpine Foreland. Tectonophysics, 137: 77-92.

BATHURST, R. G. C.: Carbonate sediments and their diagenesis: Robin G. C. Bathurst, 2nd ed. Amsterdam: Elsevier, 1975.

BADER, K., MEYER, R.K.F. & BRUNOLD, H. (2003): Die Struktur des Landshut-Neuöttinger Hochs von Mainburg bis Neumarkt-St. Veit nach seismischen Messungen und Bohrungen. Mit 11 Abb. im Text.- Geol. Bl. NO-Bayern **53**, 1-4: 1-44.

BIRNER, J. (2013): Hydrogeologisches Modell des Malmaquifers im Süddeutschen Molassebecken. – Dissertation, Freie Universität Berlin, 84 S.; Berlin.

BÖHM, F., KOCH, R., HÖFERLE, R. & BAASCH, R. (2010): Der Malm in der Geothermiebohrung Pullach Th2 — Faziesanalyse aus Spülproben (München, S-Deutschland).- Geol. Bl. NO-Bayern **60**, 1-4: 79-112.

BÖHM, F., BIRNER, J., STEINER, U., KOCH, R., SOBOTT, R., SCHNEIDER, M. & WANG, A. (2011): Tafelbankiger Dolomit in der Kernbohrung Moosburg SC4: Ein Schlüssel zum Verständnis der Zuflussraten in Geothermiebohrungen des Malm Aquifers (Östliches Molasse-Becken, Malm d-z, Süddeutschland). Z. geol. Wiss., 39, 117-157, Berlin.

BEICHEL, K, KOCH, R & WOLFGRAMM, M. (2014): Die Analyse von Spülproben zur Lokalisierung von Zuflusszonen in Geothermiebohrungen. Beispiel der Bohrungen Gt Unterhaching 1/1a und 2 (Süddeutschland, Molassebecken, Malm).- Geol. Bl. NO-Bayern 64, 1-4 & 65,1: 43-65, 12 Abb., 2 Tab.

CRAMER, H. (1953): Thermalwasser aus tiefliegenden Karsthöhlen des Bayerischen Innviertels. – Geologica Bavarica, 17: 164-177, München.

DICKSON, J. A. & COLEMAN, M. L. (1980): Changes in carbon and oxygen isotope composition during limestone diagenesis. Sedimentology, 27: 107-118.

ELBERSKIRCH, W. & LEMCKE, K. (1953): Zur Tektonik der nordalpinen Molassesenke, Z. deutschen Geologischen Gesellschaft, 105, 307-323, 3 Abb..

FOX, J., WEISSBERG, S., ADLER, D., BATES, D., BAUD-BOVY, G., ELLISON, S., ... & HEIDBERGR, R. (2012). Package 'car'. Vienna: R Foundation for Statistical Computing.

FRITZER, T. (2010): Südbayerisches Molassabecken. - In: Bayerisches Staatsministerium für Wirtschaft, Infrastruktur, Verkehr und Technologie (Hrsg.): Bayerischer Geothermie Atlas: 168-187, München.

HAN, L.-F., PLUMMER, L. N. & AGGARWAL, P. (2012): A graphical method to evaluate predominant geochemical processes occurring in groundwater systems for radiocarbon dating, Chemical Geology, 318–319, 88-112.

KOCH, R. & MUNNECKE, A. (2016): Fazielle Entwicklung und Korrelation des Oberjura in den Bohrung Bad Waldsee GB2 und Altensteig 1 (Süddeutschland; Molasse-Becken; Impressmergel- bis Hangende Bankkalk-Formation).- Geol. Bl. NO-Bayern 66, 1-4: 165-203, 8 Abb., 1 Tab., 8 Taf.

KOCH, R., BACHMANN G.H. & MÜLLER M. (2010): Fazies des Oberen Jura (Malm) der Bohrungen Scherstetten 1 und 2 (Molasse-Becken, Süddeutschland) und ihre Bedeutung für die geothermische Exploration. – Zeitschrift für geol. Wissenschaften 38 (5-6): 327–351.

KRÖNER, F., KOCH, R. & MUNNECKE, M. (2017): Aufschlussmodelle zur Fazies-Interpretation des Oberjura im östlichen Molasse-Becken (Workshop und Exkursion; 7. und 8. August 2017; Erlangen).- Geol. Bl. NO-Bayern **67**, 1-4: 167-208, 13 Abb. und 6 Taf.

LEMCKE, K. (1977): Erdölgeologisch wichtige Vorgänge in der Erdgeschichte des süddeutschen Alpenvorlandes. – Erdoel-erdgas Zeitschrift 93: 50 – 56.

LEMCKE, K. (1987): Zur Frage der alten Verkarstung des Malm im Untergrund des deutschen Molassebeckens und an dessen Nordwestrand. – Bulletin der Vereinigung der schweizerischen Petroleum-Geologen und Ingenieure 53: 33-46.

LEMCKE, K. & TUNN, W. (1956): Tiefenwasser in der suddeutschen Molasse und in ihrer verkarsteten Malmunterlage. – Bulletin der Vereinigung der schweizerischen Petroleum-Geologen und Ingenieure 23 (64): 35-56.

MEYER, R.K.F. (1996): Der Jura. In: Bayerisches Geologisches Landesamt (Hrsg): Geologischen Karte von Bayern 1:500.000. – Bayerisches Geologisches Landesamt, München.

MEYER, R.K.F. (1994): „Moosburg 4“, die erste Kernbohrung durch den Malm unter der bayerischen Molasse. – Erlanger Geologische Abhandlungen 123: 51–81.

MEYER, R.K.F. & Schmidt-Kaler, H. (1989): Paläogeographischer Atlas des süddeutschen Oberjura (Malm). – Geologisches Jahrbuch, A 115: 3–77.

NIEBUHR, B. & PÜRNER, T. (2014): Plattenkalk und Frankendolomit – Lithostratigraphie der Weißjura-Gruppe der Frankenalb (außeralpiner Oberjura, Bayern) (Beitrag zur Stratigraphie von Deutschland). – Schriftenreihe der Deutschen Gesellschaft für Geowissenschaften 83: 5–71.

NOWAK, M.E., SCHWAB, V.F., LAZAR, C.S., BEHRENDT, T., KOHLHEPP, B., TOTSCHE, K.U., KÜSEL, K. & TRUMBORE, S.E. (2017): Carbon isotopes of dissolved inorganic carbon reflect utilization of different carbon sources by microbial communities in two aquifer assemblages. – Hydrology and Earth System Sciences, 21: 4283–4300.

NOWAK, M., SMAJGL, D. & MANDIC, M. (2018): Carbon and oxygen isotope analyses by mid-infrared laser spectroscopy as a tool for stratigraphic classification of Upper Jurassic carbonate rocks. Thermo Fisher White Paper, 1-9.

R Core Team (2013): R: A language and environment for statistical computing. R Foundation for Statistical Computing, Vienna, Austria. URL: http://www.R-project.org/

REINHOLD, C. (1998). Multiple episodes of dolomitization and dolomite recrystallization during shallow burial in Upper Jurassic shelf carbonates: eastern Swabian Alb, Southern Germany. – Sedimentary Geology 121: 71–95.

ROSENBAUM, J. & SHEPPARD, S.M.F. (1988): An isotopic study of siderites, dolomites and ankerites at high temperatures. Geochimica et Cosmochimica Acta 50: 1147–1150.

RUF, M., LINK, E., PROSS, J. & AIGNER, T. (2005): Integrated sequence stratigraphy: Facies, stable isotope and palynofacies analysis in a deeper epicontinental carbonate ramp (Late Jurassic, SW Germany). - Sedimentary Geology 175: 391–414.

STÜCKL, E. (2012): "Die Urnaab Hauptrinne" (R. Meyer und K. Bader, 1998) und einige ihrer Probleme.- Geol. Bl. NO-Bayern 53, 1-4: 51-64.

TAMERS, M. A., STIPP, J. J. & WEINER, R. (1975): Radiocarbon Ages of Ground-Water as a Basis for Determination of Safe Limits of Aquifer Exploitation, Environmental Research, 9, 250-264.

UNGER, H.J. (1996): Molassebecken. – In: Bayerisches Geologisches Landesamt (Hrsg.): Erläuterungen zur Geologischen Karte von Bayern 1:500.000 (4. Aufl.): 265-266, München.

WEISSERT, H. & ERBA, E. (2004): Volcanism, CO_2 and paleoclimate: a Late Jurassic–Early Cretaceous carbon and oxygen isotope record. - Journal of the Geological Society 161: 1–8.

WIGLEY, T. M. L. (1976): Effect of Mineral Precipitation on Isotopic Composition and C-14 Dating of Groundwater, Nature, 263, 219-221.

Bayerisches Landesamt für Umwelt, Hans-Högn-Straße 12, 95030 Hof
martin.nowak@lfu.bayern.de